3D Dynamic Rupture Modeling with Depth-dependent Stress using Nonlocal Continuum Damage Breakage Rheology (Poster #194)

Chunhui Zhao[1]; Ahmed Elbanna[2,3]; Yehuda Ben-Zion[2,3]

[1]University of Illinois at Urbana-Champaign (chunhui3@Illinois.edu), [2]University of Southern California, [3]Statewide California Earthquake Center

U.S. National Science Foundation

1. Abstract

Understanding the **interplay of earthquakes and off-fault damage** is crucial for understanding earthquake processes and **linking surface observations to deformations at depth**. Numerical earthquake models still face significant challenges in capturing the fundamental mechanics of faulting and rupture.

We leverage a **three-dimensional nonlocal continuum damage–breakage model (CDBM) [2]** with **depth-dependent stress conditions and/or seismic properties distribution**, quantify differences in rupture dynamics, off-fault damage, energy partitioning and high-frequency seismic radiation.

2. Methodology

Boundary value problem

$$\nabla \cdot \sigma + f = \rho \frac{\partial^2 u}{\partial x^2} \quad in \quad V$$
$$\sigma \cdot n = T \quad on \quad S_T$$
$$u = u_o \quad on \quad S_u$$
$$T^{f+} + T^{f-} = 0 \quad on \quad S_f$$

On-Fault Friction

Slip weakening friction

$$\tau = C_o + \mu \max(0, \sigma_n - P_f)$$
$$\mu = \mu_s + (\mu_d - \mu_s) \max(f_1, f_2)$$
$$f_1 = \begin{cases} \frac{D}{d_0}, & D < D_c, \\ 1, & D \geq D_c, \end{cases} \quad f_2 = \begin{cases} 0, & t < T \\ (t-T)/t_0, & T \leq t \leq T + t_0, \\ 1, & t \geq T + t_0 \end{cases}$$

Cohesion

$$C_0 = \begin{cases} 0.40 \text{ MPa} + (0.00072 \text{ MPa/m})(5000 \text{ m} - \text{depth}), & \text{if depth} \leq 5000 \text{ m}, \\ 0.40 \text{ MPa}, & \text{if depth} \geq 5000 \text{ m}. \end{cases}$$

Nucleation

$$T = \begin{cases} \frac{r}{0.7 V_s} + \frac{0.081 r_{crit}}{0.7 V_s} \left(\frac{1}{1 - (r/r_{crit})^2} - 1 \right), & r < r_{crit}, \\ 1.0 \times 10^9 \text{ s}, & r \geq r_{crit}, \end{cases}$$

Off-Fault Rheology

Free energy

$$\Psi(T, \epsilon^e_{ij}, \alpha, \nabla\alpha, B) = (1-B)\,\Psi_S(T, \epsilon^e_{ij}, \alpha, \nabla\alpha) + B\,\Psi_B(T, \epsilon^e_{ij})$$
$$\Psi_S = \rho\left(\tfrac{1}{2}\lambda I_1^2 + \mu I_2 - \gamma I_1 \sqrt{I_2}\right)$$
$$\Psi_B = \rho\left(a_0 I_1 + a_1 I_1 \sqrt{I_2} + a_2 I_1^2 + a_3 \frac{I_1^3}{\sqrt{I_2}}\right)$$

Modulus update $\lambda = \lambda_o; \quad \mu(\alpha) = \mu_o + \alpha\xi_o\gamma_r; \quad \gamma(\alpha) = \alpha\gamma_r$

Flow Rule $\frac{d\epsilon^p_{ij}}{dt} = C_g B^{m_1} \tau^{m_2} \quad (\epsilon^t = \epsilon^e + \epsilon^p)$

Integral nonlocal strain invariant ratio

$$\hat{\xi}(x) = \frac{1}{V_r(x)} \int_V \alpha(s-x)\,\xi(x)\,dV(s),$$

Damage/breakage evolution

$$\frac{\partial(\alpha, B)}{\partial t} = \begin{cases} ((1-B)\,C_d\,I_2\,(\hat{\xi}(x) - \xi_o),\; C_B\,P(\alpha)\,(1-B)\,I_2\,(\hat{\xi}(x) - \xi_o)), & \hat{\xi}(x) \geq \xi_o, \\ ((1-B)\,C_1\,e^{\alpha/C_2}\,I_2\,(\hat{\xi}(x) - \xi_o),\; C_{BH}\,I_2\,(\hat{\xi}(x) - \xi_o)), & \hat{\xi}(x) < \xi_o. \end{cases}$$

The C_d relates to equivalent deviatoric stress rate $\dot{\epsilon}_d$:

$$C_d(\dot{\epsilon}_d) = \hat{C}_d \times \exp[1 + m \log_{10}(\frac{\dot{\epsilon}_d}{\hat{\dot{\epsilon}}})]$$

3. Problem Setup

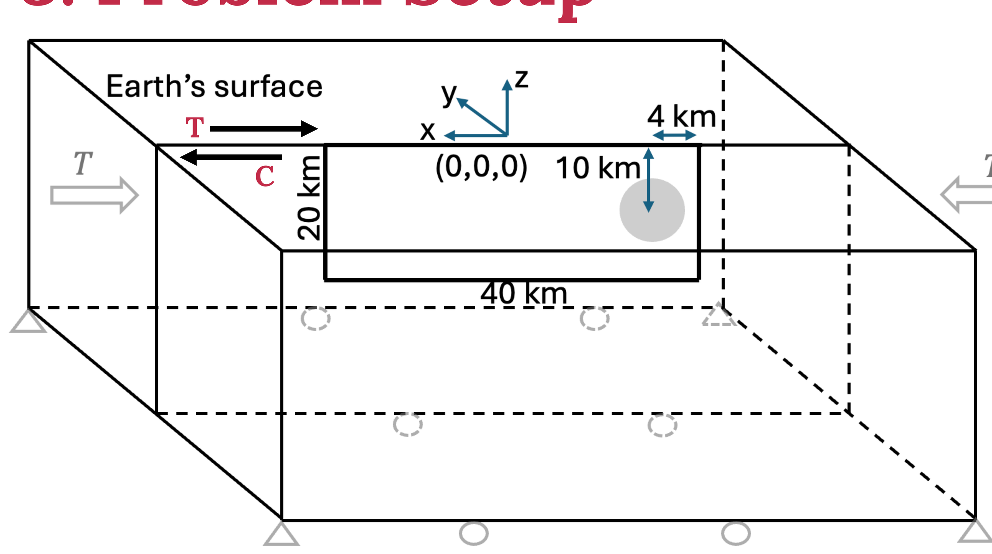

Figure: Sketch of simulation domain, Boundary conditions and nucleation sites

Static solve

$$\nabla \cdot \sigma(\epsilon - \epsilon_o) + \rho g z = 0 \; in \; V$$
$$\sigma \cdot n = T_o$$

3. Problem Setup (cont.) Depth-dependent stress/seismic properties

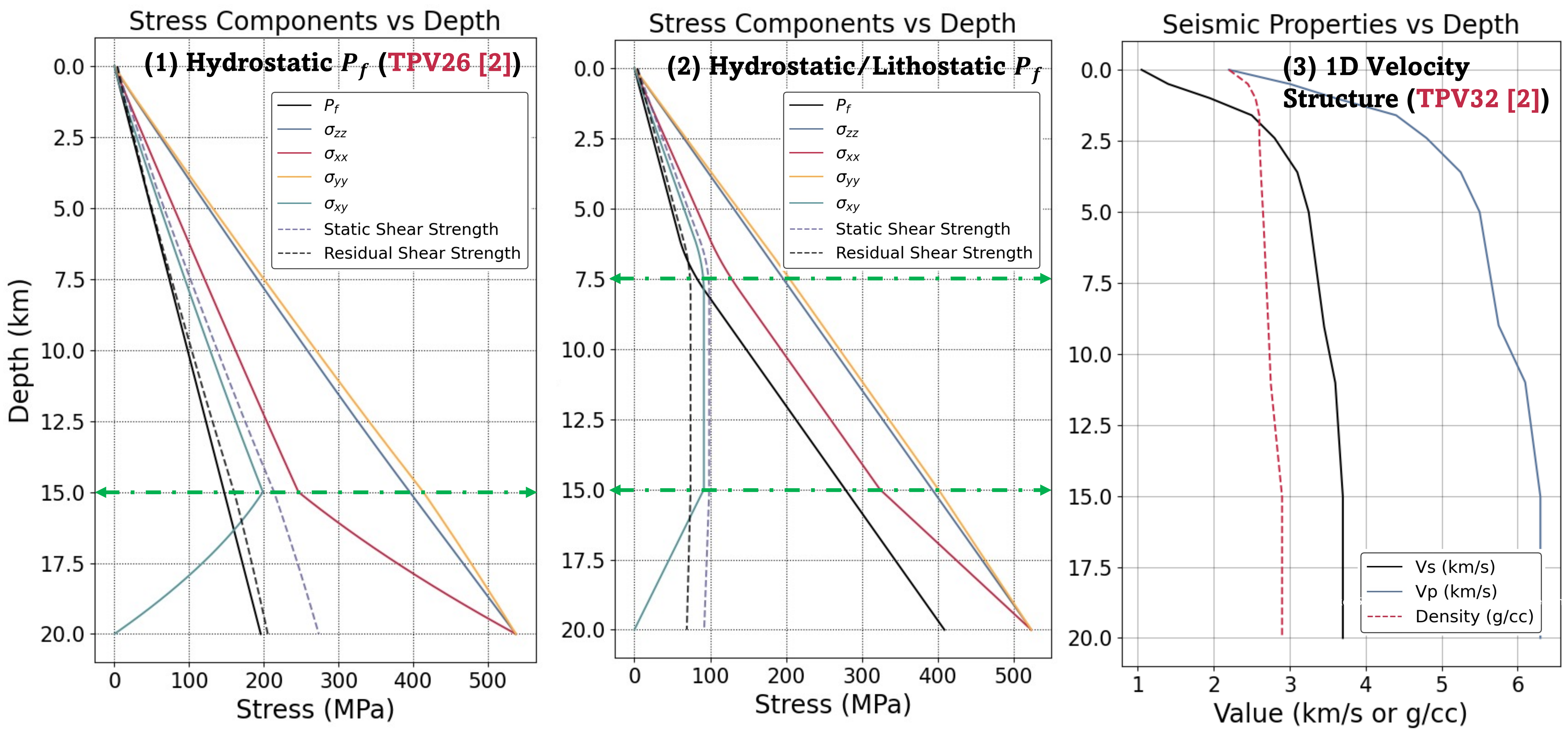

Parameter Table

Parameter Name	Value
Density ρ	2670 kg/m^3
First lamé constant λ	32.04 GPa
Shear modulus μ	32.04 GPa
Slip weakening characteristic length scale (D_c)	0.8 m
Slip weakening static friction coefficient (μ_s)	0.8
Slip weakening dynamic friction coefficient (μ_d)	0.6
Strain invariant ratio (onset of damage) (ξ_o)	-1.0
Strain invariant ratio (onset of breakage) (ξ_d)	-1.0
Coefficient of reference damage accumulation rate $\hat{C}_d$	10 1/s
Coefficient of reference strain rate $\hat{\dot{\epsilon}}$	varying
Coefficient of fitting parameter m	0.8
Multiplier between C_d and C_b	100
Coefficient of healing for breakage evolution (C_{BH})	0 1/s
Coefficient of healing for damage evolution (C_1)	0
Coefficient of healing for damage evolution (C_2)	0.05
Coefficient gives width of transitional region (β)	0.05
Compliance or fluidity of the fine grain granular material (C_g)	10^{-12}
Coefficient of power law indexes (m_1)	10
Coefficient of power law indexes (m_2)	1
Ratio of two energy state (χ)	0.8
Length of fault plane along strike (L_s)	40 km
Length of fault plane along dip (L_d)	20 km
Coefficients of depth-dependent stress (b_{xx}, b_{yy}, b_{xy})	0.4, 1.073206, -0.8
Critical nucleation radius r_{crit}	4 km
Critical strength reduction time t_o	0.5 s
Time step size (Δt)	0.005 s
End time for simulation	12 s

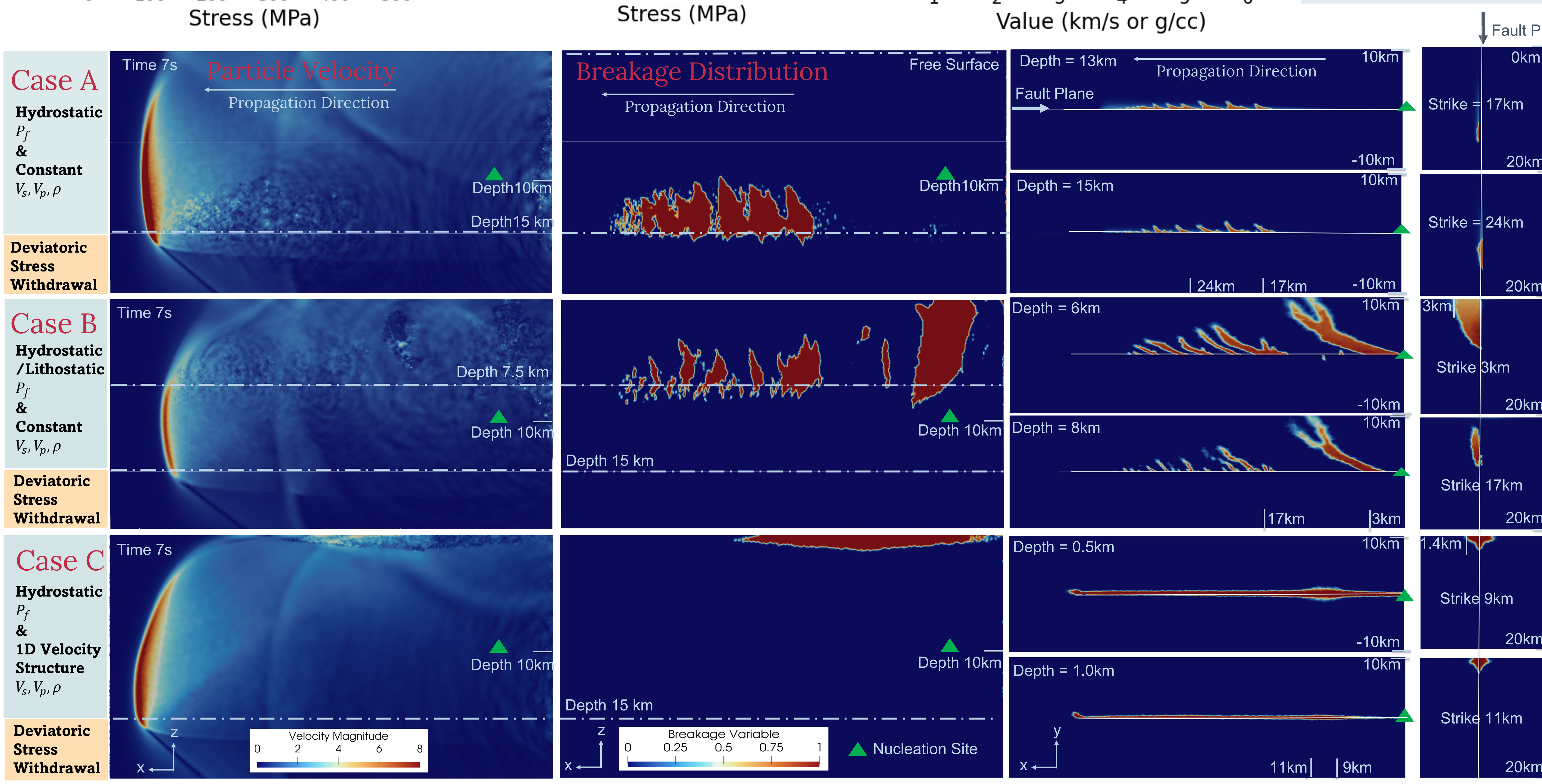

4. Results

- The code **verify against TPV26 [2]** and able to capture complex depth-dependent properties in a fully 3D setting, revealing key features on rupture dynamics and off-fault damage.
- Depth dependence: Stress states and seismic properties significantly influence rupture evolution and damage generation.
- Case A & B: Discrete off-fault damage bands form, consistent with earlier 2D plane-strain results [5], recent 3D studies [4] and 2D in plane analyses [1].
- Case B: On-fault particle velocities show a plateau in damage–breakage evolution, slightly reducing rupture speed as energy is contributed to generate damage and breakage [1]
- Case B: Off-fault receivers near the free surface record enhanced high-frequency content (1–10 Hz), consistent with [4].
- Case C: Near-surface off-fault damage develops a funnel-shaped zone, in agreement with field observations [6] and recent work [1].

5. Future Work

- Investigate the effects on hydro-mechanical coupling, temperature variation, dilatancy on rupture dynamics and damage generation
- Relate the damage generation, high frequency data to field observations, provide guidance on detecting and capturing the depth-variation of damage zone structure

Case B Rupture Dynamics Analysis

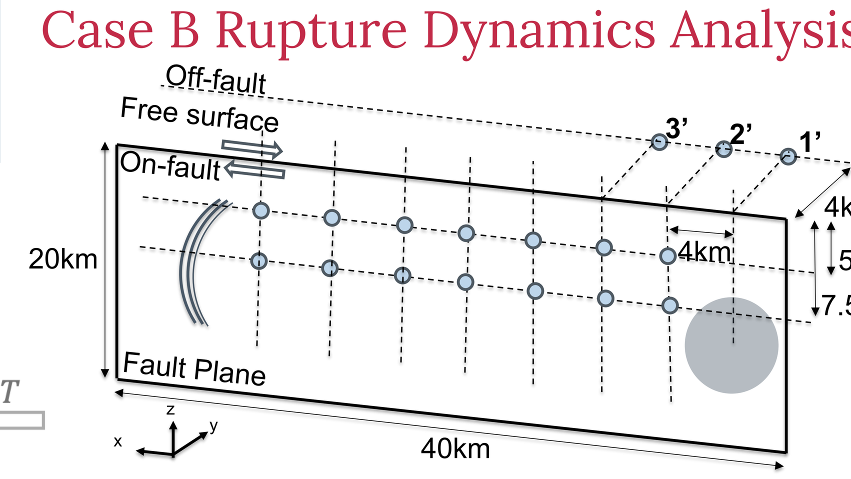

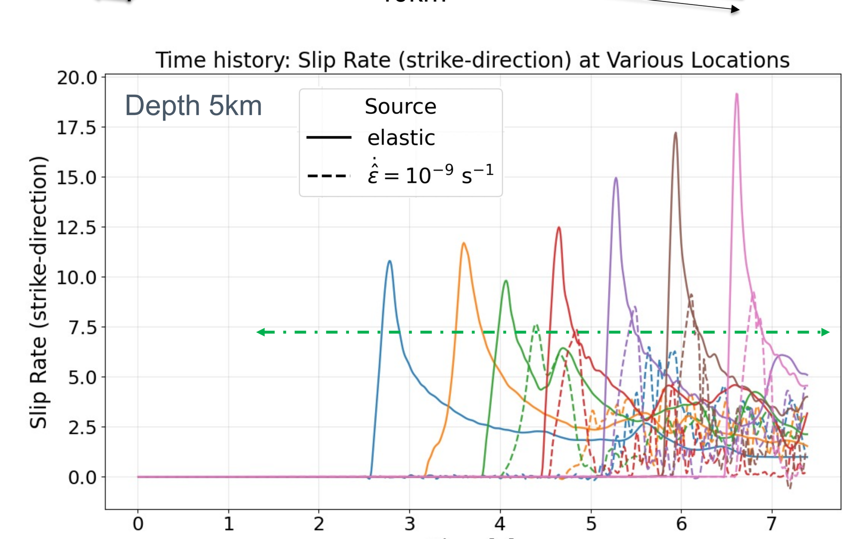

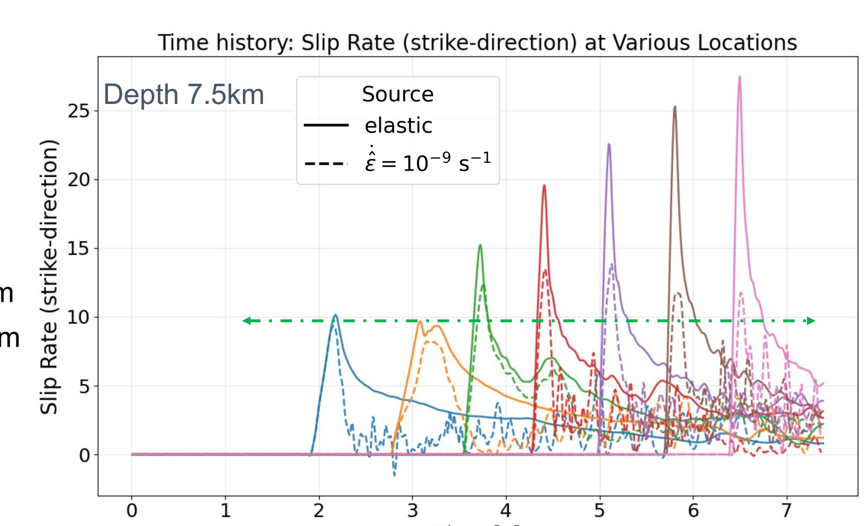

SCAN ME FOR VIDEOS!

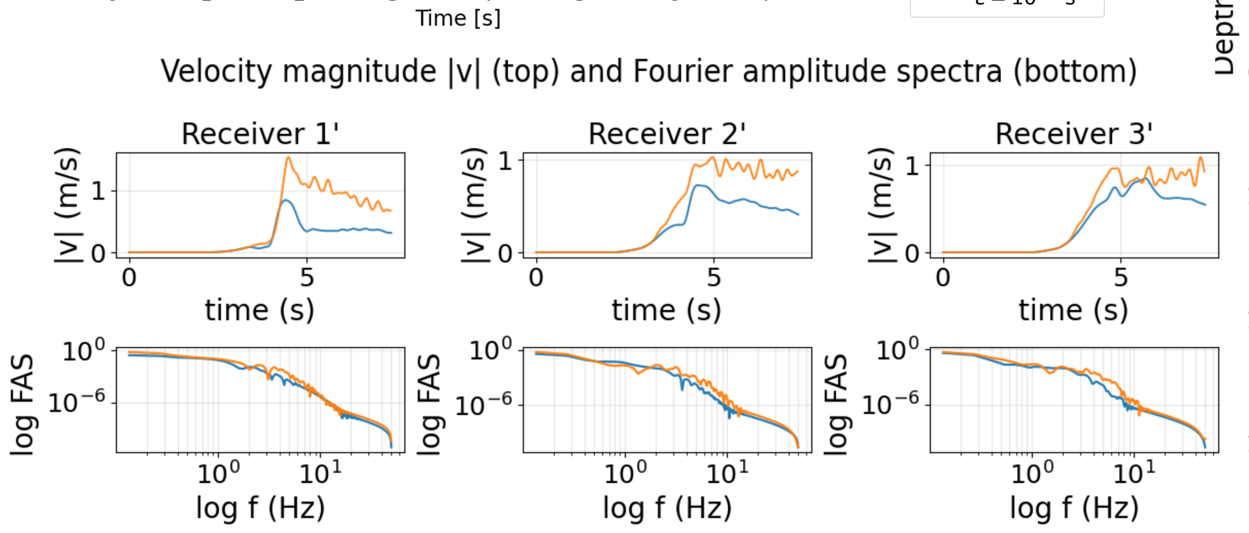

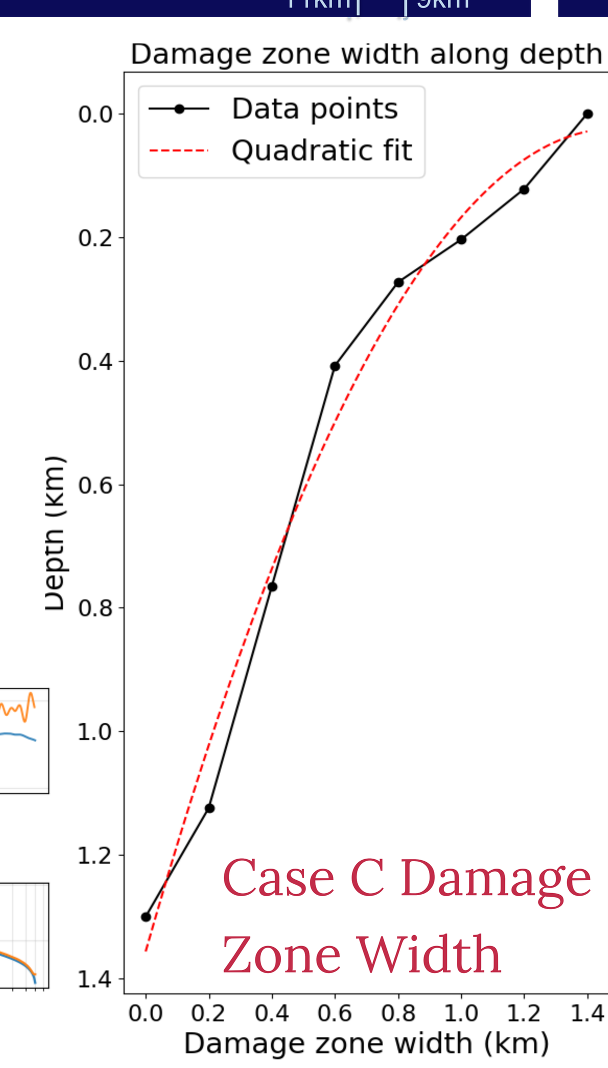

6. References

[1] Ferry, R., Thomas, M. Y., Bhat, H. S., & Dubernet, P. (2025). Depth dependence of coseismic off-fault damage and its effects on rupture dynamics. *Journal of Geophysical Research: Solid Earth*, *130*(2), e2024JB029787.
[2] Harris, R.A., M. Barall, B. Aagaard, S. Ma, D. Roten, K. Olsen, B. Duan, B. Luo, D. Liu, K. Bai, J.-P. Ampuero, Y. Kaneko, A.-A. Gabriel, K. Duru, T. Ulrich, S. Wollherr, Z. Shi, E. Dunham, S. Bydlon, Z. Zhang, X. Chen, S.N. Somala, C. Pelties, J. Tago, V.M. Cruz-Atienza, J. Kozdon, E. Daub, K. Aslam, Y. Kase, K. Withers, and L. Dalguer, A Suite of Exercises for Verifying Dynamic Earthquake Rupture Codes, Seismological Research Letters, 89(3), 1146-1162, doi:10.1785/0220170222, 2018.
[3] Lyakhovsky, V., Ben-Zion, Y., Ilchev, A., & Mendecki, A. (2016). Dynamic rupture in a damage-breakage rheology model. *Geophysical Journal International*, *206*(2), 1126-1143.
[4] Niu, Z., Gabriel, A. A., & Ben-Zion, Y. (2025). Delayed dynamic triggering and enhanced high-frequency seismic radiation due to brittle rock damage in 3D multi-fault rupture simulations. *arXiv preprint arXiv:2503.21260*.
[5] Zhao, C., Mia, M. S., Elbanna, A., & Ben-Zion, Y. (2024). Dynamic rupture modeling in a complex fault zone with distributed and localized damage. *Mechanics of Materials*, *198*, 105139.
[6] Huang, L., & Liu, C. Y. (2017). Three types of flower structures in a divergent-wrench fault zone. *Journal of Geophysical Research: Solid Earth*, *122*(12), 10-478.

7. Acknowledgements

- The simulators developed in this study are available (to-be available) on the **QUAKEWORX** science gateway for democratizing access to earthquake simulations and data.
- This research made use of the resources of the High-Performance Computing Center at Idaho National Laboratory, which is supported by the Office of Nuclear Energy of the U.S. Department of Energy and the Nuclear Science User Facilities under Contract No. DE-AC07-05ID14517.
- The authors acknowledge the Texas Advanced Computing Center (TACC) at The University of Texas at Austin for providing computational resources that have contributed to the research results reported within this paper